

## Chemical Reactivity and Covalent-Metallic Bonding of $\text{Si}_n^+$ ( $n = 11-25$ ) Clusters

James R. Chelikowsky

*Department of Chemical Engineering and Materials Science, Minnesota Supercomputer Institute,  
University of Minnesota, Minneapolis, Minnesota 55455*

J. C. Phillips

*AT&T Bell Laboratories, Murray Hill, New Jersey 07974*

(Received 11 August 1989)

Using our earlier thermodynamic force field we have calculated the equilibrium structures of medium-size  $\text{Si}_n$  clusters ( $n=11-25$ ). We find the very surprising result that beginning at  $n=7$ , near  $n=13$  and near  $n=19$ , these clusters follow a pentagonal growth pattern (icosahedra plus associated face capping). Our results are fully consistent with magic numbers recently found in the reaction rates for addition of first  $\text{C}_2\text{H}_4$  molecules to  $\text{Si}_n^+$  clusters.

PACS numbers: 81.30.-t, 82.20.Wt, 82.30.Nr

Vapor-phase clusters of  $\text{Si}_n^+$  have been prepared and analyzed for trends in relative abundance<sup>1</sup> and chemical reactivity<sup>2</sup> for  $3 \leq n \leq 60$  or 24, respectively. Magic numbers (extrema) for these properties are observed which presumably reflect differences in cluster structures. Here we show how these magic numbers can be understood based on structures predicted by a thermodynamic classical force field<sup>3</sup> developed by us to fit the equations of state of bulk phases<sup>4</sup> and energies and average coordination numbers<sup>5,6</sup> of small clusters of Si. As we anticipated,<sup>3</sup> our classical method becomes quite accurate for  $n > 10$ . First-principles quantum-mechanical calculations<sup>5,6</sup> have successfully predicted the structures and properties of  $\text{Si}_n^+$  clusters for  $n \leq 10$ .

Covalent-metallic phase transitions are the key to the functional form used to construct our force field. The analytic details of the force field are the same as those described previously,<sup>3</sup> and the values of the parameters have not been changed. The primary reason for the stability of our theory, as compared to the kaleidoscopic variations in analytic detail and parametric values which have characterized almost all other work,<sup>7-15</sup> is that our treatment of bond-bending forces is physically consistent. We use a novel angular cutoff which means that bond-bending forces are strong only for smaller bond angles, in parallel with the usual radial cutoff, which makes radial forces strong only for nearer neighbors. Moreover, our bond-bending angular function is  $\cos 3\theta$ , not  $\cos\theta$ , because the former provides the rapid angular variation needed to describe the "phase transition" between metallic ( $\theta=60^\circ$ ) and covalent ( $\theta=110^\circ$ ) bonding.

In Fig. 1 we show our results for the bulk phases<sup>4</sup> of Si. In our previous work<sup>3</sup> we fitted our parameters for the bulk energy to the equations of state for the covalent diamond and metallic simple, body-centered and face-centered cubic phases. In this figure we show, in addition, the results for the metallic hexagonal close-packed and semimetallic  $\beta$ -Sn phases with both our functions and our parameters *unchanged*. The sign and magnitude of the very small fcc-hcp difference agrees very well with

the calculation of Chang and Cohen,<sup>4</sup> also shown in the figure. This confirms the accuracy of our cutoff functions. Of greater importance to our central theme, the metal-semiconductor transition, is the excellence of the

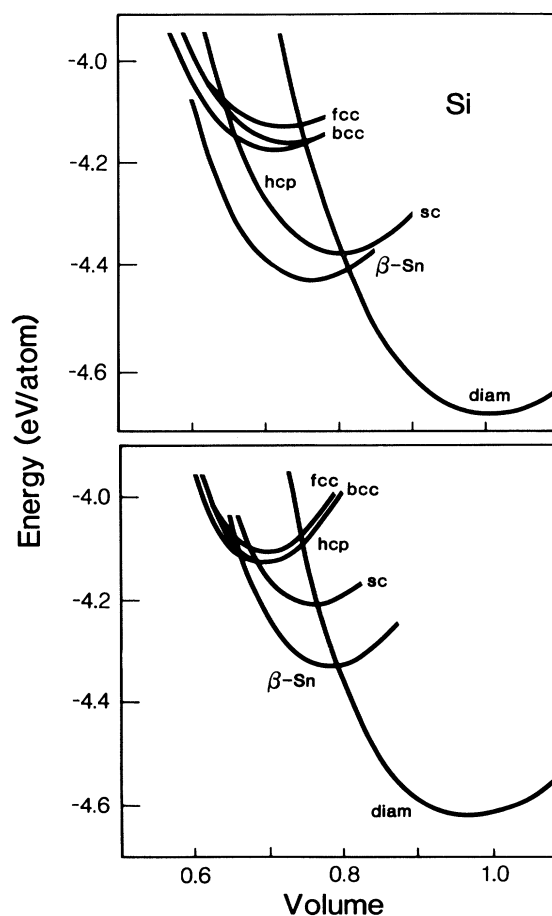


FIG. 1. We compare our results (below) for the equations of state for crystalline phases of Si with those calculated (above) by first-principles methods (Ref. 4).

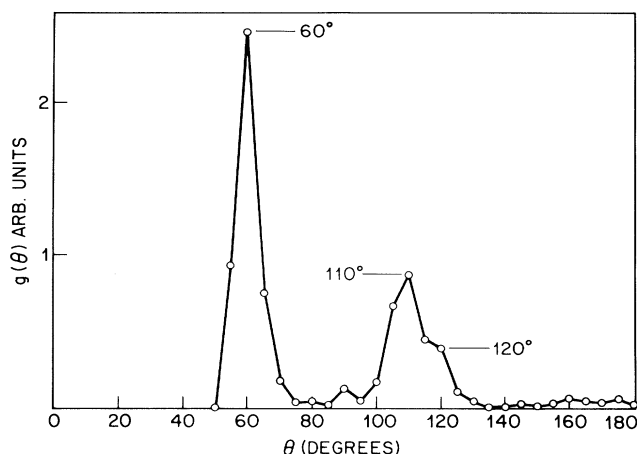


FIG. 2. Distribution of smaller bond angles in  $\text{Si}_n$  clusters ( $n=3-20$ ), as calculated by our method. Note that almost all the bond angles lie either at the metallic ( $\theta=60^\circ$ ) or covalent ( $\theta \geq \theta_t = 110^\circ$ ) limits.

unadjusted fit to the equation of state for  $\beta\text{-Sn}$ .

We now turn to the structure of  $\text{Si}_n$  clusters for  $10 \leq n \leq 25$ . These were determined by a combination of Monte Carlo and molecular-dynamics techniques.<sup>16,17</sup> The latter has been partially optimized and is now essentially as effective as such simulations<sup>12,13</sup> using much simpler potentials,<sup>7</sup> so that our practical upper limit for  $n$  is much larger than 25. However, the structures of the clusters with  $3 \leq n \leq 23$  already show striking properties which have immediate application to chemical reactivities.

First, we show in Fig. 2 the smaller bond-angle distribution for all clusters in the range  $3 \leq n \leq 20$ . While previous potentials based on  $\cos\theta$  were always *designed* to favor tetrahedral angles  $\theta_t$  [usually trivially through a term in the energy proportional to  $(\cos\theta - \cos\theta_t)^2$ ], there is no such bias in our functions.<sup>3</sup> Instead what we see in Fig. 2 is that the smaller bond angles are all concentrated near  $\theta = \pi/3$  (close packing) or near  $\theta_t$  (tetrahedral packing). This is what one would have expected from a bond-bending energy dependent on  $\cos 3\theta$ , but the virtual absence of bond angles near  $\pi/2$  reflects, in addition, certain geometrical constraints which one might not have anticipated. These packing constraints in effect amplify the significance of the covalent-metallic distinction.

For  $n > 10$ , the cluster geometries turn out to be very different from what one might have expected, based on the bulk phase diagram (Fig. 1). At  $n=13$  the structure is that of an atom-centered icosahedron. This structure, which can be described as composed of 1-5-1-5-1 layers, is the second element of a pentagonal growth sequence<sup>18</sup> which began with  $n=7$  (the bicapped 1-5-1 pentagon) and which leads to the double icosahedron 1-5-1-5-1-5-1 at  $n=19$ . Several clusters from this sequence are shown in Fig. 3. Note the regular addition of capping atoms<sup>18</sup> at  $n=14, 15$ , or 20, etc.

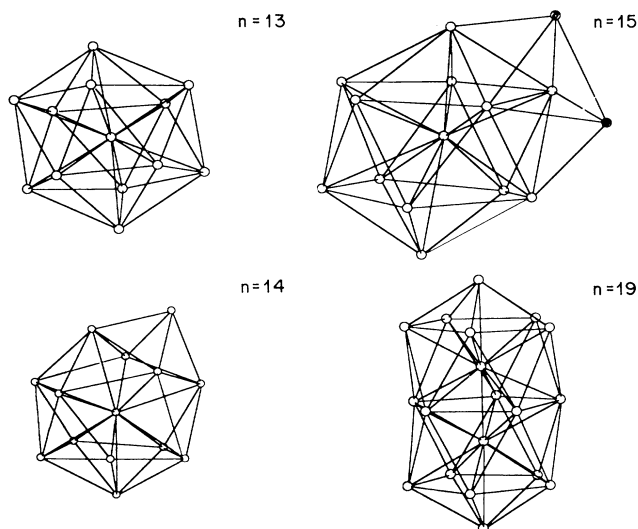


FIG. 3. Pentagonal growth clusters for several values of  $n$ , as obtained from our model. For  $n=15$ , the atoms denoted in the text by  $\text{Si}^*$  are shaded.

The icosahedral-pentagonal growth sequence is well known for two-body central forces<sup>18</sup> appropriate to inert gases, and indeed magic numbers  $n=13, 19, 23$  or  $25, \dots, 55$ , etc., have been observed for Xe and other inert-gas clusters.<sup>19</sup> However, to generate the phase diagram of Fig. 1, large three-body forces are required as well. Our calculations show that back-bonding forces<sup>3</sup> in small clusters can cause a remarkable reappearance of these simple geometrical structures.

Our model also shows for a wide range of parameters that at  $n=11, 12, 16, 17$ , and  $18$  the clusters do *not* belong to the pentagonal growth sequence but may instead have layered character similar to that of one of the  $n=10$  isomers<sup>6</sup> which has a 3-3-3-1 trigonal prismatic structure. For instance, we find  $n=16$  corresponds to 1-6-1-6-2.

We now turn to recent experimental data which apparently vindicate the main features of our results. The size dependence<sup>2</sup> of the rate constant for the addition of the first  $\text{C}_2\text{H}_4$  molecule on to  $\text{Si}_n^+$  is shown in Fig. 4. For  $n \leq 12$ , the rate constant  $k_2$  is an erratic function of  $n$ , as expected from the variety of cluster geometries calculated for  $n \leq 10$  by molecular-orbital methods.<sup>5</sup> For  $n \geq 13$  and  $n \geq 19$  smooth rises in  $k_2$  are observed. These are indicative of a common core with a repeated building block, in other words, a geometric growth sequence. The nonreactive minima at  $n=13, 19$ , and  $23$  correspond to the icosahedron, the face-capped or double icosahedron, and edge-sharing two-face-capped icosahedron. It is clear that uncapped or completely capped icosahedra containing only fivefold-coordinated atoms have minimal reactivities, whereas the  $\text{C}_2\text{H}_4$  molecules will react when there are at least two nearest-neighbor

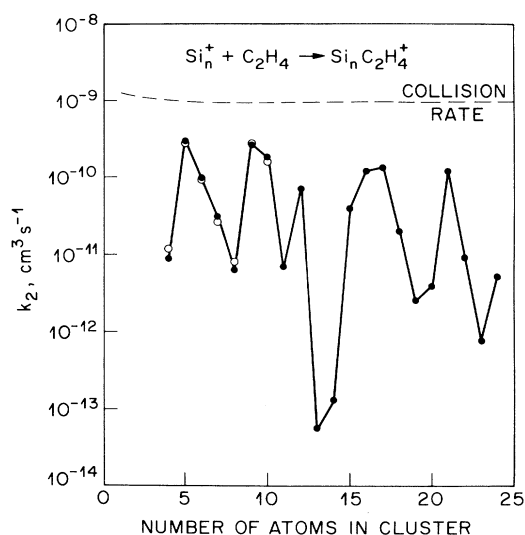


FIG. 4. Rate constants for the addition of the first  $C_2H_4$  to  $Si_n^+$ , as reported in Ref. 2 and reproduced here for the reader's convenience.

fourfold-coordinated adatoms. Denoting these adatoms by  $Si^*$ , the reactive configuration is apparently the bridge  $Si^*-H-CH=CH-H-Si^*$ . The  $C_2H_4$  reactivity with one  $Si^*$  adatom is little more than with none.

Our results indicate that in the range  $n=10-20$ , the  $Si_n$  cluster structures oscillate between metallic pentagonal growth structures and covalent molecular structures. In effect, in this range  $Si_n$  clusters are vicinal to a covalent-metallic "phase transition." It may well be that in the addition reaction the covalent molecule  $C_2H_4$  remains intact and reacts strongly only with fully covalent  $Si_n$  structures ( $n=10$  and  $16$ ) and much more weakly with metallic structures ( $n=13$  and  $19$ ). This appears to be a case of "like prefers like," which often occurs in covalent network structures. This preference originates from the persistence of the covalent energy gap, accompanied by phase-matched occupied valence orbitals, from the rings of  $Si_n$  into interlocking rings including  $C_2H_4$  segments. In earlier days this phenomenon was sometimes described as resonating valence bonds, in which case large capture cross sections near  $n=16$  could also be described as resonant addition.

Our model also yields relative cluster energies and it predicts that  $n=13$  will be especially stable. However, careful studies<sup>20</sup> of the effect of ionizing laser energy and intensity on beam distributions have revealed many effects (including cluster fragmentation, which is likely to be especially strong for "metallic" clusters) which preclude inference of relative cluster energies from beam distribution intensities in cases where the ionization energies (here known<sup>20</sup> to be  $\geq 7$  eV) are large. This makes the data shown in Fig. 4 relatively more informative, because the addition reaction is nondestructive.

Until first-principles calculations of medium-size clusters become available, it is difficult to say how accurate our model is in calculating small energy differences between covalent and metallic structures for a given  $n$ . We have, however, varied the magnitude of our back-bonding parameters over as much as a factor of 2 and have found that our qualitative conclusions remain unchanged. Thus, while our model cannot yet treat these small energy differences, it has achieved the goal expected of a classical model, that is, it generates plausible candidate structures suitable for first-principles calculations. At present (and for the foreseeable future) it appears that the first-principle methods themselves<sup>5,6</sup> encounter formidable difficulties at just this point. Thus our classical method complements the more fundamental atomic orbital<sup>5</sup> and pseudopotential<sup>6</sup> quantum calculations.

In conclusion, we have shown that without any adjustments whatsoever our previously published force field<sup>3</sup> gives an excellent fit to the equations of state of two additional crystalline phases. It also predicts very surprising pentagonal growth structures for clusters in the range  $n=13-25$ . These structures partially explain magic numbers recently observed experimentally<sup>2</sup> in the addition reaction of  $C_2H_4$  with  $Si_n^+$ . We believe that these successes demonstrate that we have constructed the first satisfactory classical model for interatomic forces for any element which is not an inert gas.

One of us (J.R.C.) would like to acknowledge support by Department of Energy Grant No. DE-FG02-89ER-45391 and the Minnesota Supercomputer Institute.

<sup>1</sup>Y. Liu, Q.-L. Zhang, F. K. Tittel, and R. E. Smalley, *J. Chem. Phys.* **85**, 7434 (1986); J. C. Phillips, *J. Chem. Phys.* **89**, 2090 (1988).

<sup>2</sup>M. F. Jarrold, J. E. Bower, and K. Creegan, *J. Chem. Phys.* **90**, 3615 (1989).

<sup>3</sup>J. R. Chelikowsky, J. C. Phillips, M. Kamal, and M. Strauss, *Phys. Rev. Lett.* **62**, 292 (1989).

<sup>4</sup>M. T. Yin and M. L. Cohen, *Phys. Rev. B* **26**, 5668 (1982); K. J. Chang and M. L. Cohen, *Phys. Rev. B* **31**, 7819 (1985).

<sup>5</sup>K. Raghavachari, *J. Chem. Phys.* **83**, 3520 (1985); **84**, 5672 (1986); K. Raghavachari and C. M. Rohlfing, *J. Chem. Phys.* **89**, 2219 (1988).

<sup>6</sup>P. Ballone, W. Andreoni, R. Car, and M. Parinello, *Phys. Rev. Lett.* **60**, 271 (1988).

<sup>7</sup>F. Stillinger and T. Weber, *Phys. Rev. B* **31**, 5262 (1985).

<sup>8</sup>R. Biswas and D. R. Hamann, *Phys. Rev. Lett.* **55**, 2001 (1985); *Phys. Rev. B* **36**, 6434 (1987).

<sup>9</sup>J. Tersoff, *Phys. Rev. Lett.* **56**, 632 (1986).

<sup>10</sup>B. W. Dodson, *Phys. Rev. B* **35**, 2795 (1987).

<sup>11</sup>M. I. Baskes, *Phys. Rev. Lett.* **59**, 2666 (1987).

<sup>12</sup>E. Blaisten-Barojas and D. Levesque, *Phys. Rev. B* **34**, 3910 (1986).

- 
- <sup>13</sup>B. Feuston, R. K. Kalia, and P. Vashista, *Phys. Rev. B* **37**, 6297 (1988).
- <sup>14</sup>S. Saito, S. Ohnishi, and S. Sugano, *Phys. Rev. B* **33**, 7036 (1986).
- <sup>15</sup>C. H. Patterson and R. P. Messmer (unpublished).
- <sup>16</sup>J. C. Tully, G. H. Gilmer, and M. Shugard, *J. Chem. Phys.* **71**, 1630 (1979).
- <sup>17</sup>M. P. Allen, *Mol. Phys.* **40**, 1073 (1980).
- <sup>18</sup>M. R. Hoare and P. Pal, *Adv. Phys.* **20**, 161 (1971).
- <sup>19</sup>J. C. Phillips, *Chem. Rev.* **86**, 619 (1986).
- <sup>20</sup>D. J. Trevor, D. M. Cox, K. C. Reichmann, R. O. Brickman, and A. Kaldor, *J. Inorg. Chem.* **91**, 2598 (1987).